Since January 2020 Elsevier has created a COVID-19 resource centre with free information in English and Mandarin on the novel coronavirus COVID-19. The COVID-19 resource centre is hosted on Elsevier Connect, the company's public news and information website.

Virology 444 (2013) 64–70

Contents lists available at ScienceDirect

Virology

journal homepage: www.elsevier.com/locate/yviro

Characterization of the polyadenylation activity in a replicase complex from *Bamboo mosaic virus*-infected *Nicotiana benthamiana* plants

I-Hsuan Chen [a], Jai-Hong Cheng [a], Ying-Wen Huang [a], Na-Sheng Lin [b], Yau-Heiu Hsu [a,c], Ching-Hsiu Tsai [a,c,*]

[a] Graduate Institute of Biotechnology, National Chung Hsing University, Taichung, Taiwan
[b] The Institute of Plant and Microbial Biology, Academia Sinica, Taipei 115, Taiwan
[c] Graduate Institute of Medical Laboratory Science and Biotechnology, China Medical University, Taichung, Taiwan

ARTICLE INFO

Article history:
Received 2 April 2013
Returned to author for revisions
20 May 2013
Accepted 22 May 2013
Available online 13 June 2013

Keywords:
BaMV
In vitro polyadenylation
Replicase
Poly(A) length
Polyadenylation signal
In vitro
Replication assay

ABSTRACT

Bamboo mosaic virus (BaMV) has a positive-sense single-stranded RNA genome with a 5′ cap and a 3′ poly (A) tail. To characterize polyadenylation activity in the BaMV replicase complex, we performed the *in vitro* polyadenylation with various BaMV templates. We conducted a polyadenylation activity assay for BaMV RNA by using a partially purified BaMV replicase complex. The results showed that approximately 200 adenylates at the 3′ end of the RNA were generated on the endogenous RNA templates. Specific fractions derived from uninfected *Nicotiana benthamiana* plants enhanced the polyadenylation activity, implying that host factors are involved in polyadenylation. Furthermore, polyadenylation can be detected in newly synthesized plus-strand RNA *in vitro* when using the exogenous BaMV minus-strand minigenome. For polyadenylation on the exogenous plus-strand minigenome, the 3′ end requires at least 4A to reach 22% polyadenylation activity. The results indicate that the BaMV replicase complex recognizes the 3′ end of BaMV for polyadenylation.

Introduction

Bamboo mosaic virus (BaMV), which is a member of the *Potexvirus* group (Lin et al., 1992, 1994), has a single-stranded positive-sense RNA genome with a 5′m^{7}GpppG structure (Lin et al., 1994) and a 3 poly (A) stretch of approximately 150 to 300 adenylates (Chen et al., 2005). The 3′ untranslated region (UTR) of the BaMV RNA folds into a series of stem-loops, including a tertiary pseudoknot structure (Tsai et al., 1999). These stem-loops in the 3′ UTR, including the binding site for RNA-dependent RNA polymerase (RdRp), are involved in the accumulation, minus-strand RNA initiation, polyadenylation, and long-distance movement of viral RNA (Chen et al., 2002, 2003, 2005; Huang et al., 2001; Tsai et al., 1999).

Polyadenylation modification is a signal for the accelerated degradation of RNA in prokaryotes (Sarkar, 1997), chloroplasts (Kudla et al., 1996; Lisitsky et al., 1996) and mitochondria (Chang and Tong, 2012). In contrast, poly(A) tails play an important role in mRNA translation and turnover (Proudfoot, 2011; Sachs and Wahle, 1993; Weill et al., 2012) and the movement of mRNA from the nucleus to the cytoplasm in eukaryotes (Huang and Carmichael, 1996; Millevoi and Vagner, 2010). For positive-sense RNA viruses, poly(A) tails have been implicated in RNA stability, translation (Bergamini et al., 2000), and replication (Guilford et al., 1991; Tsai et al., 1999). A positive correlation between the length of the poly (A)-tail and virus infectivity has been reported for several viruses including BaMV (Tsai et al., 1999), *White clover mosaic virus* (Guilford et al., 1991), poliovirus (Sarnow, 1989) and *Cowpea mosaic virus* (Eggen et al., 1989). Furthermore, the 3′ poly(A) sequences of several positive-sense RNA viruses, such as bovine coronavirus (Spagnolo and Hogue, 2000) and BaMV (Lin et al., 2007), interact with the host proteins required for viral RNA replication.

The mechanism and elements involved in polyadenylating plus-strand BaMV RNA have to be elucidated. In eukaryotes, the polyadenylation of mRNA occurs in the nucleus. However, large numbers of positive-sense RNA viruses with a poly(A)-tailed genome complete their life cycle in the cytoplasm. Although cytoplasmic polyadenylation has been reported previously in eukaryotes, the polyadenylation activities are mainly involved in oogenesis (the early development of many animal species) and regulating the diverse forms of translational activation in the cytoplasm (Radford et al., 2008; Villalba et al., 2011).

Sequence analysis of the 5′ terminus of the BaMV minus-strand RNA synthesized both *in vitro* and *in vivo* contained predominantly 7 to 10 uridylates (from 1 to 15 U residues were reported),

* Corresponding author. Fax: +886 4 2286 0260.
E-mail address: chtsai1@dragon.nchu.edu.tw (C.-H. Tsai).

0042-6822/$ - see front matter © 2013 Elsevier Inc. All rights reserved.
http://dx.doi.org/10.1016/j.virol.2013.05.032

indicating that the minus-strand RNA synthesis is initiated at approximately the 7th to 10th adenylate downstream from the 3′ UTR of the genomic RNA (Cheng et al., 2002). Accordingly, only 7 to 10 adenylates at the 3′ end of the plus-strand RNA are initially synthesized from the minus-strand RNA template during viral replication. The 3′ UTR of BaMV RNA also contains a polyadenylation signal (AAUAAA) commonly found in eukaryotic mRNA. The polyadenylation signal in the 3′ UTR of BaMV was shown to be involved in the synthesis of minus-strand viral RNA and regulating the length of the poly(A) tail (Chen et al., 2005).

In this study, we established a polyadenylation activity assay using a partially purified BaMV replicase complex isolated from virus-infected plants. Polyadenylation was detected on plus-strand RNAs synthesized from endogenous and exogenous RNA templates in this assay. Furthermore, the effects of host plant extracts on polyadenylation and the 3′ sequence of the polyadenylated RNA products were analyzed. Models of the mechanism for BaMV RNA polyadenylation are proposed and discussed in this paper.

Results

BaMV replicase complex polyadenylates endogenous RNA templates in vitro

We have demonstrated that a crude membrane-bound replicase complex isolated from BaMV-infected *N. benthamiana* plants could generate genomic and subgenomic RNAs from endogenous BaMV RNA templates (Cheng et al., 2001; Lin et al., 2005). In this study, we test whether the same extract contains the polyadenylation activity. For a polyadenylation activity assay, RNA products synthesized from endogenous RNA were labeled with radioactive [α-^{32}P] ATP during RNA replication and subsequently analyzed based on digestion with the RNase A/T1 (specific on the unpaired pyrimidines and guanine, respectively) digestion (Fig. 1A). The poly(A) RNA fragments with a higher radio-labeling intensity were generated by NP40-treated replicase complex rather than by untreated replicase complex (Fig. 1B, lanes 2 and 3). The sizes of the poly(A) fragments ranged from approximately 40 to 200 nts, which is consistent with the reported 3′ poly(A) length of BaMV genomic RNA (Chen et al., 2005). All subsequent polyadenylation activity assays were conducted using NP40 solubilization.

To confirm that the radioactively labeled fragments (the poly (A) fragments) generated by RNase A/T1 digestion were polyadenylates, the replication products were labeled with either [α-^{32}P] ATP or [α-^{32}P] UTP. The smeared radioactive RNA fragments were detected in the presence of [α-^{32}P] ATP (Fig. 1C, lane 2), but not [α-^{32}P] UTP (Fig. 1C, lane 4). Furthermore, the radioactive RNA fragments generated by RNase A/T1 digestion were hybridized with oligo-dT$_{39}$ and subjected to RNase T2 (cleavage at the unpaired nucleotides) digestion (Fig. 2A). The results indicate that the treatment converted the smeared radioactively labeled RNA fragments (Fig. 2, lane 2) into a 39-base ladder (up to 195 bases) (Fig. 2, lanes 3–5). Therefore, the RNA smears detected on the gel were likely polyadenylates generated *in vitro* by the replicase complex. Overall, these results indicate that the partially purified BaMV replicase complex is capable of producing polyadenylated RNAs from endogenous RNA templates.

Host factors are involved in the polyadenylation activity of the BaMV replicase complex

The partially purified BaMV replicase complex isolated from BaMV-infected *N. benthamiana* leaves can be separated into 10 fractions (BaMV-infected fraction; BF1 to 10) in a 20% to 60% sucrose gradient (Cheng et al., 2001; Lin et al., 2005). The highest endogenous RNA polyadenylation activity was detected in BF3 (Fig. 3A, top panel, lane 2), whereas the highest RdRp activity was detected in BF3 to 5 (Fig. 3A, bottom panel). In other words, BF4 and 5 appeared to contain components of full RdRp activity but lower polyadenylation activity compared with BF3. Subsequently, BF4 and 5 were pooled together and supplemented with fractions from uninfected plants to test whether host proteins are involved in polyadenylating BaMV RNA. Soluble fraction (HS30) and NP40-solubilized membrane fractions (healthy fraction; HF1 to HF10) of uninfected *N. benthamiana* plants were added to BF4-5 to test their effects on polyadenylation activity ([α-^{32}P] ATP labeling; Fig. 3B, top panel) and RdRp activity ([α-^{32}P] UTP labeling; Fig. 3B, bottom panel) using endogenous RNA templates. Compared with standard BF4-5 (Fig. 3B, lane 2), BF4-5 supplemented with HS30 and HF1 were shown elevated polyadenylation but not RdRp activity (Fig. 3B, lane 1 and 3, respectively). These results indicate that one or more host factors are involved in the polyadenylation activity of the BaMV replicase complex.

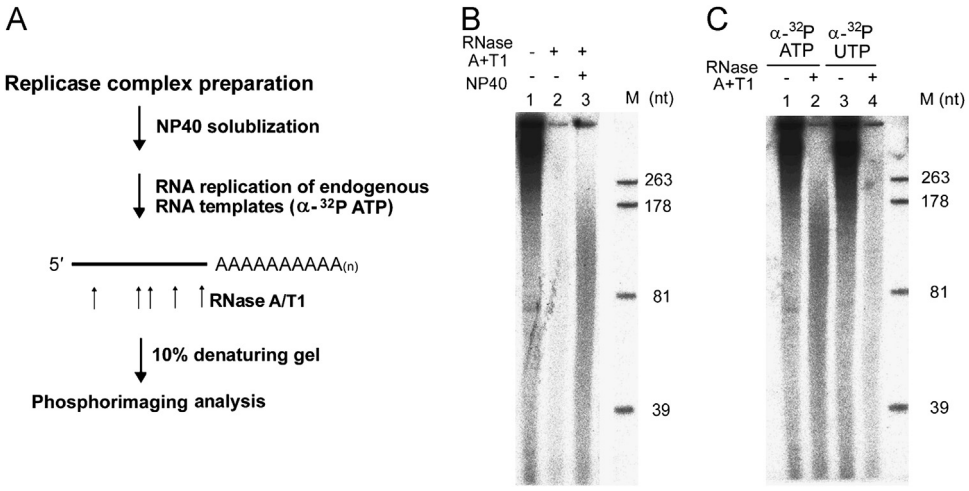

Fig. 1. Polyadenylation of endogenous RNA template-derived RNA in the *in vitro* RNA replication assay. (A) A schematic diagram showing the strategy for the polyadenylate analysis. (B) I*n vitro* BaMV RNA replication assay was carried out using untreated (lane 1 and 2) or NP40-treated (lane 3) replicase complex in the presence of [α-^{32}P] ATP. The radioactive RNA products were digested with (lanes 2 and 3) or without (lane 1) 6 μg/ml RNase A and 2000 U/ml RNase T1 in DMSO buffer. (C) RNA products were labeled with [α-^{32}P] ATP (lanes 1 and 2) or [α-^{32}P] UTP (lanes 3 and 4) in the *in vitro* RNA replication assay. The radioactive labeled products were treated with RNase A and T1 (lanes 2 and 4), analyzed on an 10% denaturing gel, and visualized by phosporimaging analysis. The sizes of ^{32}P-labeled RNA markers (M) are indicated on the right.

The addition of BaMV 3′ UTR containing the AAUAAA sequence suppresses the polyadenylation activity of the BaMV replicase complex

The AAUAAA sequence has been implicated in regulating polyadenylation efficiency in BaMV (Chen et al., 2005). To further demonstrate that the AAUAAA motif in the 3′ UTR of BaMV RNA is involved in the regulation of polyadenylation, we tested the inhibitory effects of different BaMV 3′ UTR-related RNA molecules on polyadenyaltion. RNA r138/10A contained the BaMV 3′ UTR with 10 adenylates at the 3′ end, whereas r138/10A/Δbulge and r138/10A/ΔIL were r138/10A with a bulge and an internal loop deletion, respectively, (Fig. 4) (Cheng and Tsai, 1999). The effects of the 3 RNA molecules on polyadenylation activity were evaluated in the *in vitro* replication assay. The results showed that the signal intensity of polyadenylation was largely unaffected by the addition of RNA in which the conserved AAUAAA sequence was deleted (r138/10A/ΔIL) (Fig. 4C, lane 2), but reduced and shortened in size by the RNA containing the AAUAAA motif (r138/10A and r138/10A/Δbulge) (Fig. 4C, lanes 3 and 4). It is possible that the exogenous AAUAAA motif affected polyadenylation by sequestering one or more of the polyadenylation factors in the replicase complex or by interfering directly with the enzyme complex (Chen et al., 2005).

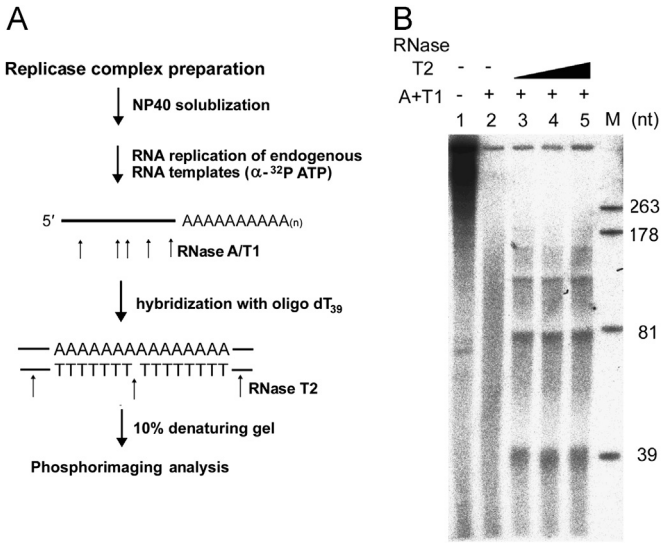

Fig. 2. Analysis of RNase A/T1-treated RNA replication products by oligo-dT_{39} priming/RNase T2 digestion. (A) A schematic diagram showing the polyadenylate analysis strategy including RNase A/T1 treatment followed by oligo-dT_{39} priming/RNase T2 digestion. (B) The radioactive RNA products from the *in vitro* RNA replication assay were incubated in the absence (lane 1) or presence of RNase A and T1 (lanes 2 to 5) in DMSO buffer. After the RNase treatment, the products were hybridized with oligo-dT_{39} and digested with increasing amounts (20, 40, and 60 U) of RNase T2 (lanes 3, 4, and 5). The products were separated on an 10% denaturing gel and visualized by phosphorimaging analysis. The sizes of ^{32}P-labeled RNA markers (M) are indicated on the right.

Polyadenylation of plus-strand BaMV RNA can be coupled with the RNA synthesis

To test whether the replicase preparation could polyadenylate exogenous plus-strand RNA templates, 5′ end-labeled radioactive BaMV plus-strand RNA substrate containing the entire 3′-UTR and 7, 15, or 40 adenylates (r138/7A, r138/15A, or r138/40A, respectively), were subjected to the polyadenylation activity assay. The results indicated that the polyadenylation signal was not detected on any of the templates in this assay (data not shown) because of inefficient polyadenylation or because the substrates were inadequate for polyadenylation. To overcome these two possible problems, we used a minigenome (a hybrid BaMV satellite/BaMV minigenome) (Huang et al., 2009) as template for RdRp assay and then performed 3′ rapid amplification of cDNA ends (3′ RACE) to analyze the 3′ terminal sequence after the reaction.

BaMV minigenomes were demonstrated to be suitable templates for an *in vitro* replication assays (Huang et al., 2009); therefore, the exogenous plus-strand or minus-strand BaMV minigenome was added to the reaction to help determine whether the poly(A) tail could be added to the 3′ end of preformed or newly transcribed plus-strand RNA, respectively. The BaMV minigenome is constructed to comprise the coding region of BaMV satellite RNA and the UTRs of BaMV. The template RNAs of the plus-strand and minus-strand minigenomes, BSM13 and BSM13(−), respectively, were prepared (Fig. 5A). The 3′ end sequences of the BSM13 templates and the plus-strand RNA products synthesized from the BSM13(−) templates were examined using 3′ RACE analysis after the

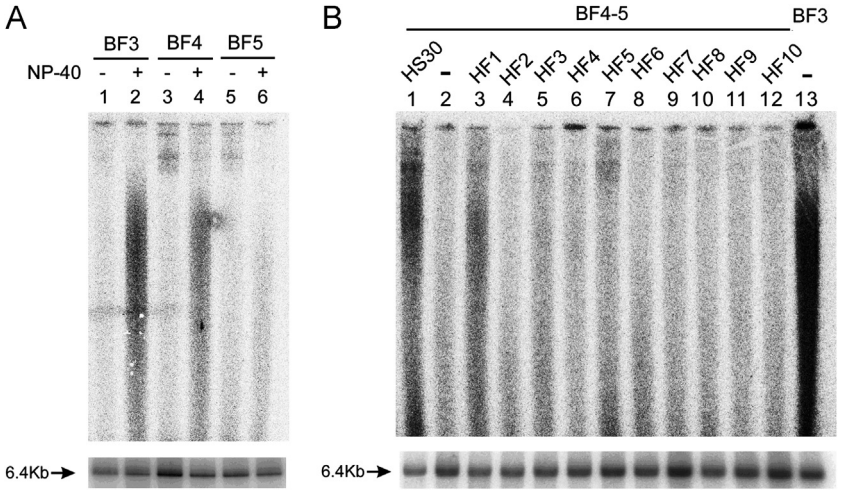

Fig. 3. Characterization of polyadenylation activity in subcellular fractions of healthy *N. benthamiana* plants. (A) Polyadenylation and RNA replication assays using fractions containing BaMV replicase complex (BF3 to 5) treated with (lanes 2, 4, and 6) or without (lanes 1, 3, and 5) NP40. (B) The soluble fraction HS30 (supernatants from 30,000 × *g* ultra-centrifugation) from healthy *N. benthamiana* plants was centrifuged through a 20–60% sucrose gradient to obtain fractions HF1 to 10 and solubilized by NP40. BF3 (lane 13) and BF4-5 (lane 2) from BaMV-infected plants, and BF4-5 supplemented with HS30 (lane 1) or HF1 to 10 (lanes 3 to 12) were subjected to polyadenylation activity (top panel) and RNA replication (bottom panel) assays. For polyadenylation assay, the RNA replication products were labeled with [α-^{32}P] ATP and digested with RNase A and T1 (top panel). The replicative form (RF) of BaMV genomic RNAs (arrow) labeled with [α-^{32}P] UTP was expected to be 6.4 kb (bottom panel). The radioactive labeled products were separated on a 1% agarose gel and visualized by phosphorimaging.

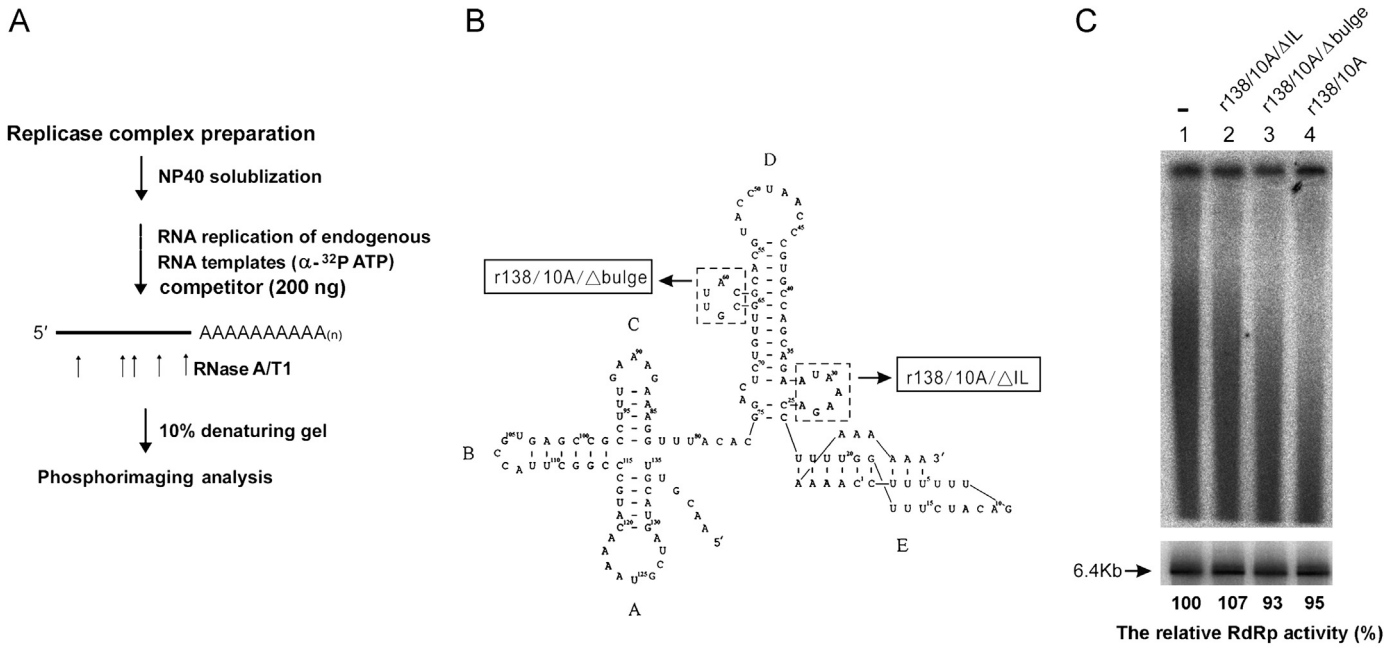

Fig. 4. Effects of synthetic 3′ UTR and mutant RNAs on BaMV RNA polyadenylation. (A) A schematic diagram showing the strategy for the polyadenylate analysis with the competitor RNAs. (B) A diagram showing the secondary structure of the r138/10A and the location of the bulge and internal loop motifs. (C) Polyadenylation assays using BF3 (lanes 1–4) were performed in the presence of a synthetic 3′ UTR transcript (r138/10A; lane 4) and its derivatives (r138/10A/Δbulge and r138/10A/ΔIL; lanes 2 and 3, respectively) as competitors (top panel). BaMV RF RNAs (arrow) generated in endogenous RNA replication assay were labeled with [α-^{32}P] UTP (bottom panel). The radioactive labeled products were separated on a 1% agarose gel and visualized and quantified by phosphorimaging. The relative accumulation levels of BaMV RNA were shown under each lane.

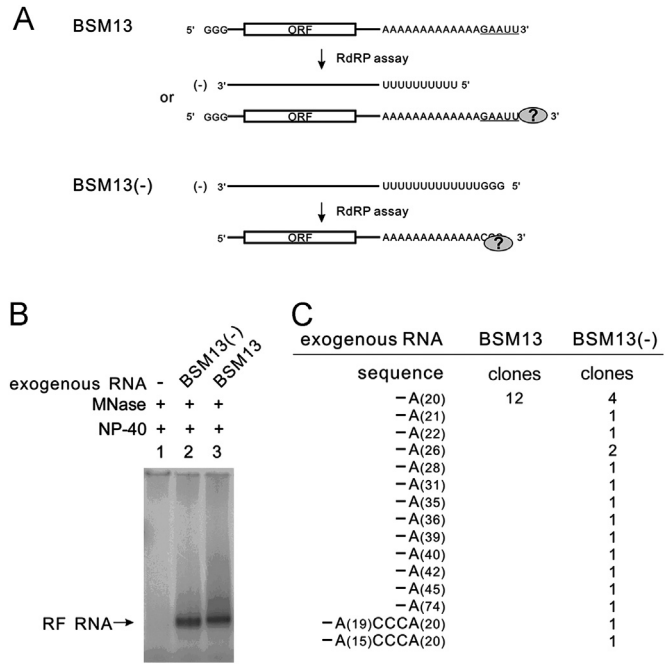

Fig. 5. Polyadenylation of exogenous and newly synthesized plus-strand RNA templates in the *in vitro* RNA replication assay. (A) A diagram illustrating the BSM13 and BSM13(−) RNAs and their possible replication products. The 3′ GAAUU sequence of BSM13 was derived from the *EcoR*I-linearized DNA template. The 5′ $(G)_3$ sequence of BSM13(−) was derived from the T7 RNA polymerase promoter. (B) Exogenous BSM13 or BSM13(−) RNA was added to the *in vitro* RNA replication assay driven by NP40-solubilized/ micrococcal nuclease-treated replicase complex. The double-stranded RF RNAs generated from BSM13(−) (lane 2) and BSM13 (lane 3) in the assay were labeled with [α-^{32}P]ATP and separated on a 1% agarose gel. (C) 3′ sequences of the RNA products shown in panel B. The RNA products were subjected to 3′ RACE analysis. DNA sequences of the 3′ RACE products were determined.

in vitro replication (Fig. 5B). The DNA sequence of 12 clones derived from the BSM13 template showed that all clones contained a 20-adenylate sequence downstream of the 3′ UTR (Fig. 5C). The 20 adenylates were possibly derived from the RACE primer dT_{20}, which can prime to the BSM13 RNA template harboring the $–A_{13}$GAAUU sequence (GAAUU is derived from *EcoR*I when preparing the run-off transcription) (Fig. 5A). The results indicate that either no or considerably few adenylates were added to the 3′ end of BSM13 RNA templates.

In contrast, the newly synthesized plus-strand RNAs derived from BSM13(−) included 20 to 74 consecutive adenylates (Fig. 5C). Because the 5′-terminal sequence of BSM13(−) is $GGGU_{13}$- (GGG is derived from the T7 promoter; Fig. 5A), the 3′-end sequence of the newly synthesized plus-strand RNA copied from the template should contain $–A_{13}$CCC. The results indicate that adenylates were added to the 3′ end of newly synthesized RNAs. Although the clones containing the polyadenylates ranging from 20 to 31 (10 clones) did not result from polyadenylation, the remaining clones with consecutive polyadenylates ranging from 35 to 74 (7 clones) did. Because the template provides 13 Us for copying and the primer dT_{20} for reverse transcription, only RNAs with active polyadenylation can have more than 33 adenylates in the clones.

In 2 clones (containing an $–A_{15/19}C_3A_{20}$ sequence), the poly (A) track is interrupted by a CCC sequence, which is derived from the template GGG. The results indicate that polyadenylation might occur before reaching the GGG sequence (only 13 uridylates in the template; Fig. 5A). However, the polyadenylation enzyme complex could return to the template and copy the G_3 sequence during polyadenylation. This could be due to the enzyme copying slippage, although the cloning artifact could not be disregarded. Overall, the results indicate that polyadenylation began before the replication enzyme complex reached the GGG sequence and that BaMV RNA replication was accompanied by an exonuclease activity in which the C_3 sequence was removed before the poly (A) tail was added.

Polyadenylation on the preformed genomic RNA requires at least 4 adenylates at the very 3′ end

In the mentioned results, we could not detect adenylates longer than 20 in all the clones derived from BSM13 after the reaction (Fig. 5C). Because BSM13 is a suitable template for minus-strand RNA synthesis, the *in vitro* reaction could be more efficient in RNA replication than in polyadenylation. To exclude minus-strand RNA synthesis from the reaction, we included only ATP and GTP in the RdRp assay. To test the requirements of the 3′ end structure for polyadenylation, we used the RNA transcripts derived from PCR products to obtain the precise sequence instead of using run-off transcripts, which contain a nonviral sequence (the *Eco*RI site). BSM13/noA, −/4A, −/7A, and −/13A templates were prepared and incubated with the BaMV replicase complex, and ATP and GTP were included in the reaction. The reaction products were examined using a head-to-tail ligation and RT-PCR analysis (Wu and Brian, 2010) instead of 3′ RACE in which the primer (dT_{20}) might cover the authentic 3′-end sequence. The sequence results indicate that no adenylate can be added to the template without a preexisting adenylate (Table 1, BSM13/noA). Long preexisting adenylates at the very 3′ end of the template (with 4, 7, and 13 As) cause efficient for polyadenylation (22%, 46%, and 68%, respectively). The results indicate that the partially purified BaMV replicase complex is capable of polyadenylating the preformed exogenous RNA templates. The RNA template required at least 4 adenylates to obtain a minimum of 22% efficiency for polyadenylation.

Discussion

The BaMV is a positive-sense RNA viruses with a poly(A)-tailed genome. The results (Figs. 1 and 2) of this study confirm that BaMV positive-sense RNA is polyadenylated. Compared with the untreated BaMV replicase complex preparation, the NP40-treated preparation resulted in enhanced poly(A) signal intensity in the products of the *in vitro* RNA replication assay (Fig. 1B). This was probably due to particular conformational changes or subunit rearrangements in the enzyme complex induced by the detergent NP40. Numerous studies have not connected the BaMV infection cycle with the nucleus. Therefore, it is unlikely that the addition of the poly(A) tail to the BaMV genome during its replication cycle is processed by the nuclear polyadenylation machinery of the host cell. Plants encode enzymes, such as nucleotidyltransferase and polynucleotide phosphorylase, for the RNA polyadenylation involved in the poly(A)-stimulated RNA degradation pathway in mitochondria and chloroplasts (Lange et al., 2009; Zimmer et al., 2009). Accordingly, the possibility that the polyadenylation of viral RNA occurs through this type of host-encoded cytoplasmic proteins cannot be disregarded.

Poly(A)-tailing of the newly synthesized plus-strand RNA from the minus-strand BaMV minigenome was clearly detected (Fig. 5), indicating that polyadenylation coupled with the plus-strand RNA synthesis is efficient and that the AAUAAA motif is accessible to the replicase complex during plus-strand RNA synthesis. In contrast, incubating exogenous plus-strand RNAs with the BaMV replicase complex does not lead to the polyadenylation of BSM13/noA RNA (Table 1), but leads to a minimal activity of approximately 22% for BSM13/4A RNA. A presence of a large number of preexisting adenylates at the 3′ end of the templates (BSM13/7A and BSM13/13A) resulted in the efficient addition of adenylates (46% and 68%, respectively; Table 1). It is possible that the 3′ UTR of BaMV is arranged in a way that the polyadenylation signal AAUAAA is hidden and not initially accessible to the enzyme complex. When the 3′ end extended with more adenylates such as 7A and 13A (copying from the templates during replication), the pseudoknot structure formed (Fig. 4B) and the AAUAAA motif was exposed for the switch from replication to polyadenylation.

When the competitor RNAs were added to the replicase preparation, RdRp activity persisted, but polyadenylation activity decreased if the competitor RNA contained the AAUAAA sequence (Fig. 4C). These results suggest that the 2 enzymatic activities (RdRp activity and polyadenylation) could be separated during BaMV replication. The plus-strand RNA copies from the minus-strand RNA template with RdRp activity until the end of the template that the plus-strand RNA forming the pseudoknot structure and exposing the AAUAAA sequence. The host factor (s) could recognize the sequence and switch to polyadenylation activity. Therefore, the competitor RNA containing the AAUAAA sequence could eliminate the host factor(s) in replicase preparation through competition.

In eukaryotes, the polyadenylation of mRNA precursors may be a two-phase process. Approximately 9 adenylates are added to the 3′ end of the RNA containing a conserved AAUAAA sequence during the first phase. Subsequently, independent of the AAUAAA motif and the associated factors, the polyadenylation complex extends efficiently from the short oligo(A) to generate a full-length poly(A) tail (approximately 200 adenylates) (Sheets and Wickens, 1989). In general, the polyadenylation process of BaMV plus-strand RNA is similar to that of eukaryotic mRNA. These similarities include the requirements of the AAUAAA motif (Chen et al., 2005), the synthesis of a short oligo(A) (derived from the minus-strand template), and the synthesis of a poly(A) tail of a similar length. BaMV minus-strand RNA synthesis was shown to initiate between the seventh to tenth adenylate abutting the 3′ UTR on plus-strand RNA (Cheng et al., 2002), leading to the presence of a few uridylates at the 5′ end of the minus-strand RNA. These uridylates in minus-strand RNA could serve as the template for the first few adenylates of the poly(A) tail on plus-strand RNA. These adenylates could be used as the primer for the synthesis of up to 300 adenylates (Chen et al., 2005). Moreover, mutation of the AAUAAA sequence in the BaMV system led to poly(A) tails of a shorter length (Chen et al., 2005), indicating that the polyadenylation complex of the BaMV replication machinery is associated with the AAUAAA motif during the tailing process.

Adding particular subcellular fractions (HS30 and HF1) from uninfected plants increased the polyadenylation activity but not

Table 1
Polyadenylation efficiency of exogenous plus-strand RNA.

Templates	Adenylates			
	Shortening < template	No editing = template	Adenylating > template	Adenylating range
BSM13/no A	0 (0%)[a]	9 (100%)	0 (0%)	0 A
BSM13/4 A	1 (6%)	13 (72%)	4 (22%)	6–18 As
BSM13/7 A	0 (0%)	7 (54%)	6 (46%)	9–13 As
BSM13/13 A	9 (29%)	1 (3%)	21 (68%)	14–35 As

[a] Data are numbers of clones, with percentages in parentheses.

the RdRp activity (Fig. 3B). Host factors are possibly responsible for regulating the switch between template-dependent RNA synthesis and the polyadenylation mode. In another possible mode of polyadenylation, the enzyme complex simply shuttles back and forth on the oligo(U) region of the template to generate the poly (A) tail, which is similar to the poly(A) tail generation process of influenza virus mRNA synthesis (Poon et al., 1999). Terminal adenyltransferase activity has been demonstrated in the nsP4 (RdRp) of Sindbis virus (Tomar et al., 2006) and the $3D^{pol}$ of poliovirus (Neufeld et al., 1994). In contrast, an internal poly (A) tract in the 3′ UTR of *Dulcamara mottle virus* (Tzanetakis et al., 2009), *Chikungunya alphavirus* (Khan et al., 2002), and *Hibiscus latent Singapore virus* (Srinivasan et al., 2005) has been proposed to lead to viral polymerase slippage during RNA replication.

The replicase complex isolated from BaMV-infected plants contains both replication activity and polyadenylation activity. These activities could be regulated with different host factor (s) and replication can switch to polyadenylation during genomic RNA synthesis.

Materials and methods

Plasmid construction

pBSM13 was constructed previously to allow *in vitro* synthesis of BSM13 RNA, a chimeric BaMV minigenome RNA containing the open reading frame from BaMV satellite RNA flanked by the 5′ and 3′ UTRs of BaMV genomic RNA (Huang et al., 2009). For *in vitro* synthesis of BSM13(−), a minus-strand BaMV minigenome RNA, pBSM13(−) was constructed from pBSM13 by PCR using the BamHI-BaMV5′+1 (5′GAATTCGAAAACCACTCCAAACGAAA3′) and T7-13T BaMV3′end (5′GGTACCTAATACGACTCACTATAGGGTTTTT-TTTTTTTTGGAAAA3′) primers. The PCR product was cloned into a *Sma*I-linearized pUC119 vector and verified by DNA sequencing analysis.

Exogenous RNA substrates

Templates for *in vitro* transcription were generated by PCR instead of restriction enzyme linearized-plasmids to get the expected 3′ ends. pBSM13 was used as the template in the PCR. The forward primer T7-BaMV5′+1 (5′GCTCTAGATAATACGACTCAC-TATAGAAAACCACTCCAAACGAA3′) and reverse primers BaMV 3′ end noA (5′GGAAAAAACTGTAGA AACCAAAAG3′), BaMV 3′end 4A (5′TTTTGGAAAA AACTGTAGAAACC3′), BaMV 3′end 7 A (5′TTT-TTTTGGAAAAAACTGTAGAAA3′), and BaMV 3′end 13A (5′TTTTTT-TTTTTTTGGAAAA3′) were generated BSM13/noA, −/4A, −/7A, and −/13A. The PCR products were gel purified and used for *in vitro* transcription by T7 RNA polymerase (Promega, Madison, WI, USA). After transcription, the mixture was treated with RQ1 RNase-Free DNase (Promega, Madison, WI, USA) at 37 °C for 30 min. Transcripts were extracted with phenol/chloroform and precipitated with ammonium acetate and ethanol. RNA concentration was determined by spectrophotometry and agarose gel electrophoresis.

In vitro BaMV RNA replication assay

BaMV replicase complex was purified from BaMV-infected *N. benthamiana* leaves as described previously (Cheng et al., 2001; Lin et al., 2005). In brief, the healthy and BaMV infected leaves were kept in −80 °C. The frozen leaves were homogenized in RdRp complex extraction buffer (50 mM Tris–HCl pH 7.6, 15 mM $MgCl_2$, 120 mM KCl, 0.1% β-mercaptoethanol, 20% glycerol, 1 μM pepstatin A, 0.1 mM phenylmethenylsulphonyl fluoride). The homogenate was filtrated through Miracloth (CalBiochem) and centrifuged at 500 × *g* for 10 min to remove the cell debris. The clarified supernatant was applied to a 30,000 × *g* ultra-centrifugation for 35 min, and the pellet (P30) was re-suspended in solubilization buffer (50 mM Tris–HCl pH 8.2, 10 mM $MgCl_2$, 1 mM dithiothreitol, 1 μM pepstatin A, 1 μM leupeptin). The 50-μl BaMV RNA replication assay containing 20 μl of 1.5% NP40-solubilized replicase fractions (Cheng et al., 2001), 4.8 mg/ml bentonite, 10 mM dithiothreitol, 10 mM $MgCl_2$, 2 μM ATP, 0.066 μM [α-^{32}P]-ATP (3000 Ci/mmol, Dupont-NEN, Boston, MA), and 2 mM UTP, CTP, and GTP was carried out at 30 °C for 1 h. For labeling with [α-^{32}P]-UTP, the concentrations of UTP and ATP were changed to 2 μM and 2 mM, respectively. The RNA products were extracted with phenol/chloroform and precipitated with ethanol. For assays using exogenous templates, NP40-treated BaMV replicase complex was treated with micrococcal nuclease (USB Corporation, Cleveland, OH, USA) and the reaction stopped by adding 30 mM EGTA before the addition of the RNA template (1 μg).

For the competitor RNAs, the cDNA fragments containing the 3′ UTR of BaMV and its derivatives were PCR amplified with the primer set, T7-BaMV+6228 (5′GCGAATTCTAATACGACTCACTATAG-GGCGTTGCATGATCG3′) and BaMV 3′end 10A (5′TTTTTTTTTTGG-AAAAAACTGTAGAAA3′), and the plasmid templates, pBaMV40A, −/ΔIL and −/Δbulge (Chen et al., 2005). These fragments were cloned into pUC18 vector with the *Sma*I site. The resultant clones, pBa138/10A, pBa138/10A/ΔIL and pBa138/10A/Δbulge, were linearized with *Bam*HI. The RNAs, r138/10A, −/ΔIL and −/Δbulge, were transcribed from these linearized plasmids and were gel-purified. In the competition RdRp assay, 200 ng of the competitor was added into the reaction.

RNase digestion assay

The radioactively labeled RNA products generated in BaMV RNA replication assay were digested with RNase A (6 μg/ml) and RNase T1 (2000 U/ml) in DMSO buffer (30.8% DMSO and 13.2 mM Tris–HCl pH 7.8) at 37 °C for 20 min. The products were extracted with phenol/chloroform, precipitated with ethanol, and dissolved in 1X urea sample buffer (4.5 M urea, 15 mM sodium-citrate pH 5.0, 0.5 mM EDTA, 0.01% xylene cyanol FF, and 0.01% bromophenol blue). The radioactively labeled RNAs were denatured in boiling water for 2 min, separated on a 10% denaturing gel and visualized by a BAS-1500 phosphorimaging analyzer (Fujifilm, Tokyo, Japan). To demonstrate the presence of poly (A) tails, the RNase A/T1-treated RNA products were incubated with oligo-$(dT)_{39}$ at 70 °C for 10 min. The mixture was cooled down to 37 °C and treated subsequently with 20, 40, and 60 U of RNase T2 in DMSO buffer at 37 °C for 20 min. The RNA products were extracted with phenol/chloroform, precipitated with ethanol, separated on a 10% denaturing polyacrylamide gel, and visualized by phosphorimaging.

3′ Race analysis

The products from polyadenylation assay were converted into cDNA by using primer OligodT_{20}/GC-clamp (5′GCCCCGGGAT-CCTTTTTTTTTTTTTTTTTTTT3′) and SuperScript III reverse transcriptase (Invitrogen, Carlsbad, CA, USA). The cDNAs were amplified by PCR for 35 cycles using forward primer BaSat+607 (5′GCTGACG-CGTGGCTCCCTGACCGTG3′) corresponding to nt 607–631 of BaMV satellite RNA, reverse primer OligodT_{20}/GC-clamp, and GoTaq® Flexi DNA Polymerase (Promega). The PCR products were cloned into the pGEM T-easy vector (Promega).

Head-to-tail ligation of viral RNA products and sequence analysis of the 3′ end RNA

RNAs extracted from i*n vitro* exogenous RNA replication assay were dephosphorylated with shrimp alkaline phosphatase (Promega, Madison, WI, USA) and followed by phosphorylation with T4 polynucleotide kinase (New England Biolabs, Beverly, MA, USA). Before head-to-tail ligation, the RNAs were denatured at 95 °C for 5 min and then quick-chilled on ice. The denatured RNAs were added to 1 μl of 10x ligase buffer and 1 U of T4 RNA ligase 1 (NEB) in a total of 10 μl reaction, and the mixture was incubated at 16 °C for 16 h. After phenol/chloroform extraction, the ligated RNAs were converted into cDNA with ImProm-II™ Reverse Transcriptase (Promega) and Ba-77 (5′GGGCGATTGTAGGGGA3′) priming at nt 62–77 in plus strand of BaMV. The cDNAs were further amplified by PCR for 35 cycles using forward primer BaSat+607, reverse primer Ba-21 (5′GTTTCGTTTGGAGTGGTT3′) corresponding to nt 4–21 of BaMV, and GoTaq® Flexi DNA Polymerase (Promega). The PCR products were sequenced after cloning into the pGEM T-easy vector (Promega).

Acknowledgments

This work was supported by grants from National Science Council (NSC 96-2752-B-005-012-PAE and 97-2752-B-005-004-PAE.

References

Bergamini, G., Preiss, T., Hentze, M.W., 2000. Picornavirus IRESes and the poly (A) tail jointly promote cap-independent translation in a mammalian cell-free system. RNA 6, 1781–1790.
Chang, J.H., Tong, L., 2012. Mitochondrial poly(A) polymerase and polyadenylation. Biochim. Biophys. Acta 1819, 992–997.
Chen, I.H., Chou, W.J., Lee, P.Y., Hsu, Y.H., Tsai, C.H., 2005. The AAUAAA motif of *Bamboo mosaic virus* RNA is involved in minus-strand RNA synthesis and plus-strand RNA polyadenylation. J. Virol. 79, 14555–14561.
Chen, I.H., Meng, M., Hsu, Y.H., Tsai, C.H., 2003. Functional analysis of the cloverleaf-like structure in the 3′ untranslated region of *Bamboo mosaic potexvirus* RNA revealed dual roles in viral RNA replication and long distance movement. Virology 315, 415–424.
Cheng, C.P., Tsai, C.H., 1999. Structural and functional analysis of the 3′ untranslated region of *Bamboo mosaic potexvirus* genomic RNA. J. Mol. Biol. 288, 555–565.
Cheng, J.H., Ding, M.P., Hsu, Y.H., Tsai, C.H., 2001. The partial purified RNA-dependent RNA polymerases from *Bamboo mosaic potexvirus* and *Potato virus X* infected plants containing the template-dependent activities. Virus Res. 80, 41–52.
Cheng, J.H., Peng, C.W., Hsu, Y.H., Tsai, C.H., 2002. The synthesis of minus-strand RNA of *Bamboo mosaic potexvirus* initiates from multiple sites within the poly (A) tail. J. Virol. 76, 6114–6120.
Eggen, R., Verver, J., Wellink, J., De Jong, A., Goldbach, R., van Kammen, A., 1989. Improvements of the infectivity of *in vitro* transcripts from cloned *Cowpea mosaic virus* cDNA: impact of terminal nucleotide sequences. Virology 173, 447–455.
Guilford, P.J., Beck, D.L., Forster, R.L., 1991. Influence of the poly(A) tail and putative polyadenylation signal on the infectivity of *White clover mosaic potexvirus*. Virology 182, 61–67.
Huang, C.Y., Huang, Y.L., Meng, M., Hsu, Y.H., Tsai, C.H., 2001. Sequences at the 3′ untranslated region of *Bamboo mosaic potexvirus* RNA interact with the viral RNA-dependent RNA polymerase. J. Virol. 75, 2818–2824.
Huang, Y., Carmichael, G.G., 1996. Role of polyadenylation in nucleocytoplasmic transport of mRNA. Mol. Cell Biol. 16, 1534–1542.
Huang, Y.W., Hu, C.C., Lin, C.A., Liu, Y.P., Tsai, C.H., Lin, N.S., Hsu, Y.H., 2009. Structural and functional analyses of the 3′ untranslated region of *Bamboo mosaic virus* satellite RNA. Virology 386, 139–153.
Khan, A.H., Morita, K., Parquet, Md, Mdel, C., Hasebe, F., Mathenge, E.G., Igarashi, A., 2002. Complete nucleotide sequence of *Chikungunya virus and evidence for an internal polyadenylation site*. J. Gen. Virol. 83, 3075–3084.
Kudla, J., Hayes, R., Gruissem, W., 1996. Polyadenylation accelerates degradation of chloroplast mRNA. EMBO J. 15, 7137–7146.
Lange, H., Sement, F.M., Canaday, J., Gagliardi, D., 2009. Polyadenylation-assisted RNA degradation processes in plants. Trends Plant Sci. 14, 497–504.
Lin, J.W., Ding, M.P., Hsu, Y.H., Tsai, C.H., 2007. Chloroplast phosphoglycerate kinase, a gluconeogenetic enzyme, is required for efficient accumulation of *Bamboo mosaic virus*. Nucleic Acids Res. 35, 424–432.
Lin, J.W., Hsu, Y.H., Tsai, C.H., 2005. Characterization of the infectivity of *Bamboo mosaic virus* with its correlation to the *in vitro* replicase activities in *Nicotiana benthamiana*. Virus Res. 112, 77–84.
Lin, N.S., Lin, B.Y., Lo, N.W., Hu, C.C., Chow, T.Y., Hsu, Y.H., 1994. Nucleotide sequence of the genomic RNA of *Bamboo mosaic potexvirus*. J. Gen. Virol. 75, 2513–2518.
Lin, N.S., Lin, F.Z., Huang, T.Y., Hsu, Y.H., 1992. Genome properties of *Bamboo mosaic virus*. Phytopathology 82, 731–734.
Lisitsky, I., Klaff, P., Schuster, G., 1996. Addition of destabilizing poly (A)-rich sequences to endonuclease cleavage sites during the degradation of chloroplast mRNA. Proc. Nat. Acad. Sci. U.S.A. 93, 13398–13403.
Millevoi, S., Vagner, S., 2010. Molecular mechanisms of eukaryotic pre-mRNA 3′ end processing regulation. Nucleic Acids Res. 38, 2757–2774.
Neufeld, K.L., Galarza, J.M., Richards, O.C., Summers, D.F., Ehrenfeld, E., 1994. Identification of terminal adenylyl transferase activity of the poliovirus polymerase 3Dpol. J. Virol. 68, 5811–5818.
Poon, L.L., Pritlove, D.C., Fodor, E., Brownlee, G.G., 1999. Direct evidence that the poly(A) tail of influenza A virus mRNA is synthesized by reiterative copying of a U track in the virion RNA template. J. Virol. 73, 3473–3476.
Proudfoot, N.J., 2011. Ending the message: poly(A) signals then and now. Genes Dev. 25, 1770–1782.
Radford, H.E., Meijer, H.A., de Moor, C.H., 2008. Translational control by cytoplasmic polyadenylation in Xenopus oocytes. Biochim. Biophys. Acta 1779, 217–229.
Sachs, A., Wahle, E., 1993. Poly(A) tail metabolism and function in eucaryotes. J. Biol. Chem. 268, 22955–22958.
Sarkar, N., 1997. Polyadenylation of mRNA in prokaryotes. Annu. Rev. Biochem. 66, 173–197.
Sarnow, P., 1989. Role of 3′-end sequences in infectivity of poliovirus transcripts made *in vitro*. J. Virol. 63, 467–470.
Sheets, M.D., Wickens, M., 1989. Two phases in the addition of a poly(A) tail. Genes Dev. 3, 1401–1412.
Spagnolo, J.F., Hogue, B.G., 2000. Host protein interactions with the 3′ end of bovine coronavirus RNA and the requirement of the poly(A) tail for coronavirus defective genome replication. J. Virol. 74, 5053–5065.
Srinivasan, K.G., Min, B.E., Ryu, K.H., Adkins, S., Wong, S.M., 2005. Determination of complete nucleotide sequence of *Hibiscus latent singapore virus*: evidence for the presence of an internal poly(A) tract. Arch. Virol. 150, 153–166.
Tomar, S., Hardy, R.W., Smith, J.L., Kuhn, R.J., 2006. Catalytic core of alphavirus nonstructural protein nsP4 possesses terminal adenylyltransferase activity. J. Virol. 80, 9962–9969.
Tsai, C.H., Cheng, C.P., Peng, C.W., Lin, B.Y., Lin, N.S., Hsu, Y.H., 1999. Sufficient length of a poly(A) tail for the formation of a potential pseudoknot is required for efficient replication of *Bamboo mosaic potexvirus* RNA. J. Virol. 73, 2703–2709.
Tzanetakis, I.E., Tsai, C.H., Martin, R.R., Dreher, T.W., 2009. A tymovirus with an atypical 3′-UTR illuminates the possibilities for 3′-UTR evolution. Virology 392, 238–245.
Villalba, A., Coll, O., Gebauer, F., 2011. Cytoplasmic polyadenylation and translational control. Curr. Opin. Genet. Dev. 21, 452–457.
Weill, L., Belloc, E., Bava, F.A., Mendez, R., 2012. Translational control by changes in poly(A) tail length: recycling mRNAs. Nat. Struct. Mol. Biol. 19, 577–585.
Wu, H.Y., Brian, D.A., 2010. Subgenomic messenger RNA amplification in coronaviruses. Proc. Nat. Acad. Sci. U.S.A. 107, 12257–12262.
Zimmer, S.L., Schein, A., Zipor, G., Stern, D.B., Schuster, G., 2009. Polyadenylation in Arabidopsis and Chlamydomonas organelles: the input of nucleotidyltransferases, poly(A) polymerases and polynucleotide phosphorylase. Plant J. 59, 88–99.